The Inclusion of Arbitrary Load Histories in the Strength Decay Model for Stress Rupture

Author: James R Reeder

ABSTRACT

Stress rupture is a failure mechanism where failures can occur after a period of time, even though the material has seen no increase in load. Carbon/epoxy composite materials have demonstrated the stress rupture failure mechanism. In a previous work, a model was proposed for stress rupture of composite overwrap pressure vessels (COPVs) and similar composite structures based on strength degradation. However, the original model was limited to constant load periods (holds) at constant load. The model was expanded in this paper to address arbitrary loading histories and specifically the inclusions of ramp loadings up to holds and back down. The broadening of the model allows for failures on loading to be treated as any other failure that may occur during testing instead of having to be treated as a special case. The inclusion of ramps can also influence the length of the "safe period" following proof loading that was previously predicted by the model. No stress rupture failures are predicted in a safe period because time is required for strength to decay from above the proof level to the lower level of loading. Although the model can predict failures during the ramp periods, no closed-form solution for the failure times could be derived. Therefore, two suggested solution techniques were proposed. Finally, the model was used to design an experiment that could detect the difference between the strength decay model and a commonly used model for stress rupture. Although these types of models are necessary to help guide experiments for stress rupture, only experimental evidence will determine how well the model may predict actual material response. If the model can be shown to be accurate, current proof loading requirements may result in predicted safe periods as long as 10^{13} years. COPVs design requirements for stress rupture may then be relaxed, allowing more efficient designs, while still maintaining an acceptable level of safety.

NOMENCLATURE

A	normalized parameter used in iterative solution for t_f
b	nonlinearity parameter in strength decay model
c	time scale parameter in strength decay model
PDF	probability density function
R	ramp rate for applied stress

$\mathbb{R}$ reliability

$s(t)$ instantaneous strength (strength of a given test specimen at some point in time)
s' derivative of strength with respect to time
s_o initial strength in a given test specimen
SR stress ratio, ratio of stress level to the strength scale parameter
$\widehat{\mathbb{S}}$ scale parameter for Weibull distribution of initial strengths
t time
t_{ref} classic model reference time to failure (scale parameter at SR=1)
α Weibull shape parameter for strength
β Weibull shape parameter for time to failure
σ stress
ρ classic model parameter for sensitivity to stress ratio

Subscripts
1 start of a load step
2 end of a load step
f failure point
i iteration count

INTRODUCTION

Stress rupture is a failure mechanism where failures can occur after a period of time, even though the material has seen no increase in load. Carbon/epoxy composite materials have demonstrated the stress rupture failure mechanism. One application where stress rupture may be critical is in Composite Overwrap Pressure Vessels (COPVs). COPVs are used in the aerospace industry to transport gases under very high pressures (e.g., 5000 psi). This application may be worse than others because the composite material tends to be uniformly loaded at elevated stress levels for prolonged periods of time. As seen in Figure 1, COPVs come in various sizes and are either cylindrical or spherical in shape. Several varieties of composite overwrap have been

Figure 1. Composite overwrap pressure vessels (COPV)

used, including Kevlar\/Epoxy, but most COPVs in current use in the aerospace

industry are made with carbon fibers. Because these critical structures operate under very high pressures, a failure of a vessel would likely lead to loss of life and/or property.

A COPV structure is made of a thin metal liner that is then wrapped with composite. To avoid stress rupture in the composite, the pressure in the COPV is normally limited to a relatively low percentage of the vessel burst pressure (typically less than 50%). Reliability models are used to predict the likelihood of stress rupture at various stress levels. By keeping the stress level in the composite low, the chance of a failure is kept acceptably small (e.g., 1 in 1 million). The reliability models are based on experimental data, but there is significant extrapolation from the reliability levels where tests can be performed to the predictions of reliabilities that are desired. For example, a test of a million vessels to show a one in a million chance of failure is not feasible. Because of the high cost of vessels, stress rupture is often tested on smaller specimens such as individual strands, which are a single tow of fiber (perhaps 1000 fiber filaments) impregnated with a polymer. These strand specimens exhibit the stress rupture phenomenon and are much cheaper test specimens than full COPVs. An example of composite stress rupture data that can be collected is presented in Figure 2 [1]. The data in Figure 2 are collected from strands and each individual point represents one failure. Different numbers of specimens were tested at each load level, and the percentage that survived the testing are noted to the right in the figure. Two things are clear from the stress rupture data presented in Figure 2: as the stress level (i.e., load) is decreased, the percentage of surviving specimens grows dramatically; and the time to failure of apparently identical test specimens under identical loading can be vastly different.

In order to make reliability predictions at lower loads where COPVs are used, data like that shown in Figure 2 are often modeled with an empirical reliability model such as the one known as the “classic model” given by eq. 1 [2, 3].

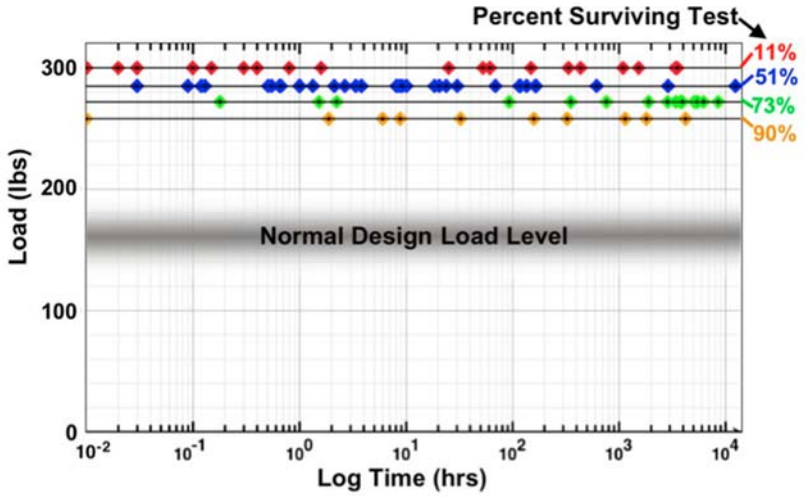

Figure 2. Time to failure data from a stress rupture study on IM6 composite test specimens[1]

$$\mathbb{R} = e^{-\left(\frac{t}{t_{ref}\left(\frac{\sigma}{\widehat{\mathbb{S}}}\right)^{-\rho}}\right)^{\beta}} \quad (1)$$

$\mathbb{R}$ is the predicted reliability for the test specimens that have been held under constant stress σ for a period of time, *t*. $\rho, \beta,$ and t_{ref} are material parameters used to fit the model to the test data. The model is scaled to the initial strength of the test specimens using the $\widehat{\mathbb{S}}$ parameter, which is the scale parameter from a Weibull distribution fit to the measured strength distribution. By normalizing the model with the strength parameter, it is assumed that the stress rupture response of a strand will be similar to that of a full vessel. The parameter $\sigma/\widehat{\mathbb{S}}$ in eq. 1 is often referred to as the stress ratio, *SR*.

Although eq. 1 is written for a constant stress level, it can be extended to any load history. To explain how the classic model predicts failures under varying stress level conditions, a "video playback" analogy will be used. A video could be recorded of the failures from a group of test specimens held at a constant stress level. Because carbon epoxy stress rupture has demonstrated a decreasing failure rate, the "playback" of the video would show several failures early in the stress period, but the rate of failures would slow overtime. Increasing the load level at any point in the testing acts as if the video playback was switched to "fast forward." The pattern of failures would stay the same, but the rate at which they occur would increase. Similarly, lowering the load would act to put the video into "slow motion" where the rate of failures would decrease. Using this video playback concept, eq. 2 predicts the failures if all the specimens were held at a reference stress level, σ_{ref}. Equation 3 translates actual time at different stress levels into effective time, t_{eff}, or the equivalent amount of time if the entire stress history had been at the reference stress level. [4].

$$\mathbb{R} = e^{-\left(\frac{t_{eff}}{t_{ref}\left(\frac{\sigma_{ref}}{\widehat{\mathbb{S}}}\right)^{-\rho}}\right)^{\beta}} \quad (2)$$

$$\text{where} \quad t_{eff} = \int_0^t \left(\frac{\sigma[t]}{\sigma_{ref}}\right)^{\rho} dt \quad (3)$$

Since σ_{ref} can be canceled out of eq. 2 once eq. 3 is substituted into the equation, the choice of the reference stress level is arbitrary and can be chosen to be the dominant level of loading during testing. At any point in time and at all stress levels, there is some chance of a failure occurring.

Other models for stress rupture have also been postulated. A much earlier work had proposed a capability degradation model, but the early work was formulated around time dependent crack growth equations instead of strength decay [5]. Yet another stress rupture model was formulated around creep in the matrix causing delayed failures in fibers that accumulate to cause specimen failure [4], but this micromechanics model is not formulated in a way that can be readily validated [6].

In a previous work by the author, a new strength decay model was proposed in which the scatter in stress rupture times was attributed to the variation in initial strengths. Strength decays over time until the strength level drops to the applied stress

level, at which point the material fails. Equation 4 shows the strength degradation law that was proposed. Constant stress level stress rupture data can be fit with the strength decay model as well as they can be fit to with the classic mode. In fact, the two models can be made to give essentially the same predictions of reliability under constant stress conditions.

$$\frac{s[t]}{\sigma} = \left(\left(\frac{s_o}{\sigma}\right)^b - \frac{t}{c}\right)^{\frac{1}{b}} \tag{4}$$

In the strength decay model, b and c are material constants. The parameter b describes the shape of the strength curve as it decays, and c scales the curve in time. The predicted reliability from the strength decay model is given by eq. 5 once the initial strength, s_o, required for a failure at a given time was determined from eq. 4 [7].

$$\mathbb{R} = e^{-\left(\frac{s_o}{\widehat{\mathbb{S}}}\right)^{\alpha}} \tag{5}$$

Equation 5 describes a Weibull distribution with a shape parameter α and a scale parameter $\widehat{\mathbb{S}}$.

To make the strength decay model produce similar reliability results to the classic model, the following strength decay parameters were used: $c=t_{ref}$, $b = \rho$ and $\alpha = \rho\,\beta$. The reliability equations are not identical in form, and there is some difference in predicted reliabilities at very short times. However, at longer times where stress rupture reliability is available, the models give essentially the same results.

Although the reliability predictions from the classic model and the decay model were quite similar for constant stress cases, the results were quite different following a proof loading where an initial elevated load level is applied to the specimen followed by a lower level of loading. In fact, the strength decay model predicted a "safe period" following the proof loading because time was required for the strength to decay from some value higher than the elevated stress level to a the lower stress level. During this safe period, no failures would be predicted. No safe period is predicted by the classic model.

In the previous derivation, the strength decay model was limited to constant stress load steps. This constraint limited the breadth of problems that could be addressed by the model. In this paper, the model will be expanded for arbitrary loading. Several implications of the expanded model will be discussed. The new expanded model will then be used to plan a test series based on a complex load history to help validate the model.

STRENTH DECAY UNDER ARBITRARY LOADING

Derivation of Strength decay law

Equation 4 was derived based on the theory that a relationship between internal strength and stress level would control the time to failure, which would occur when the strength equals the stress level. The strength is unknown for most of the life of the material and only becomes known at failure. Equation 4 was derived by working backwards from the observed reliability results and assuming a Weibull distribution of initial strengths as opposed to working forward from a governing equation. Equation 3 begins when the strength level is s_o, which implies that any previous load history

does not influence the rate of strength decay going forward. This allows eq. 4 to be recalculated for a second period at constant load. The final strength after the first period becomes the initial strength in the second, and *t* becomes the time in the second period. The original strength decay model was shown in the initial published work to have significantly different predictions of reliability following proof loading compared to the classic model [7].

Equation 4 does not hold for arbitrary loading histories. The relationship of time *t* to strength *s* in the equation assumes that the stress has been constant for the entire period. For arbitrary loading, an equation describing the change in strength is necessary, and this equation cannot be directly dependent on time. To be consistent with the earlier assumptions that the internal strength state variable is sufficient to record the past life of the composite, the instantaneous change in strength, s', can only be a function of current state variables and material parameters, as shown in eq. 6.

$$s'[t] = f[s[t], \sigma[t], b, c\,] \tag{6}$$

A governing equation for the strength decay should be of the form that satisfies eq. 6 and, when integrated over a constant load period, should recover eq. 4. Equation 7 meets these criteria.

$$s'[t] = -\frac{\sigma[t]}{bc}\left(\frac{s[t]}{\sigma[t]}\right)^{1-b} \tag{7}$$

By separating variables as shown in eq. 8 and integrating with σ remaining constant over the period, eq. 4 can be derived from eq. 7.

$$s^{b-1}\,ds = -\frac{\sigma^b[t]}{bc}\,dt \tag{8}$$

Note that just taking a derivative of eq. 4 would result in an equation for $s'[t]$ that is a function of *t*, and this would imply a history dependence, which violates earlier assumptions made in the model development.

Assuming eq. 7 as the governing equation for strength decay, the strength after any arbitrary loading can be predicted from any starting point where the current strength is known. Deriving equations for the strength decrease after specific load histories will prove to be helpful. The strength decrease during a constant stress increase from zero stress can be derived using eq. 8.

$$\int_{s_o}^{s[t]} s^{b-1}\,ds = \int_0^t -\frac{(Rt)^b}{bc}\,dt$$

$$\frac{s^b[t]-s_0^b}{b} = -\frac{(Rt)^{b+1}}{R\,(b+1)\;b\,c}$$

$$s[t] = \left(s_0^b - \frac{t(Rt)^b}{c(1+b)}\right)^{1/b} \tag{9}$$

where *R* is the ramp rate of the linearly changing stress from $\sigma = 0$, so $\sigma[t] = Rt$.

Similarly the strength at the end of a constant ramp starting at some arbitrary stress level would be

$$s[t_2] = \left(s^b[t_1] - \frac{(R(t_2-t_1)+\sigma_1)^{1+b} - (R\,t_1+\sigma_1)^{1+b}}{c(1+b)R}\right)^{1/b} \tag{10}$$

Note that R can be positive or negative depending on whether the applied stress is increasing or decreasing, and the subscript 1 implies the beginning of the load period while 2 implies the end.

Equation 4 provides the expression for a constant load case, but it is repeated here as eq. 11 with updated notation, using subscripts 1 and 2.

$$s_2 = \sigma_1 \left(\left(\frac{s_1}{\sigma_1} \right)^b - \frac{t}{c} \right)^{1/b} \tag{11}$$

With eq. 10 and 11, more complex load histories can be predicted such as that shown in Figure 3. Note that for each step t_1, s_1, σ_1 refers to the beginning of the step and t_2, s_2 and σ_2 refer to the end of the step. The material parameters used to create the figure are based on classic model parameters commonly used for the T1000/epoxy material [4], namely ρ =114, β =0.22, and t_{ref} =0.001 hr. These parameters will be the basis for all the predictions presented in this paper. As described previously, the classic model parameters correspond to the following decay model parameters: b =114, c =0.001 and α = 25.08. Note that in Figure 3, the length of time in each period is longer than typically used in testing so that the decay pattern can be more easily seen. Normally, ramps would be faster, and the hold during proof loading would be shorter.

Equation 10 was generated for a linear ramp, but other loading cases could also be derived from eq. 7 such as a logarithmic or parabolic load step. Although other types of steps are possible, the ramp and constant load steps can be combined to provide reliability predictions for a large number of practical problems.

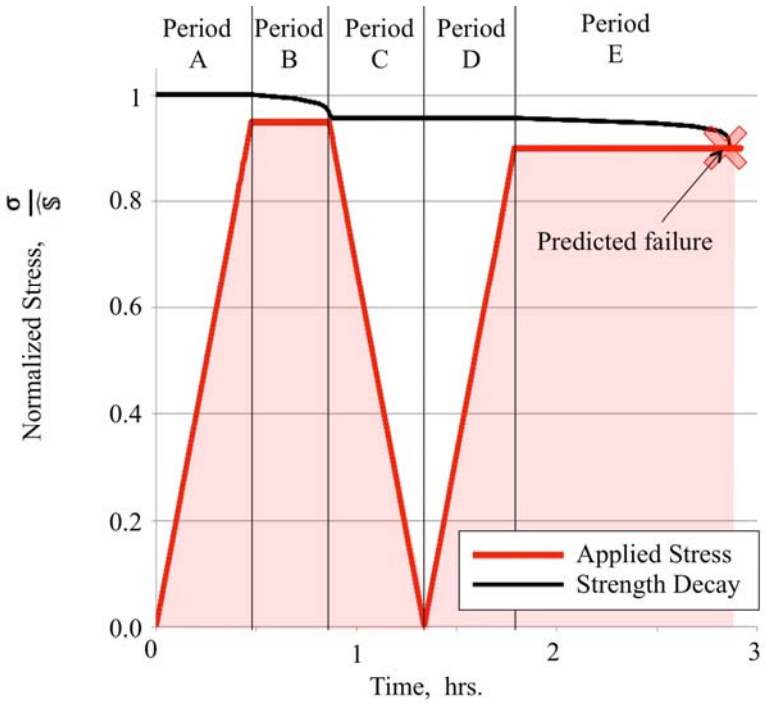

Figure 3. Strength decay with complex load history

Time to Failure

In using a model like the strength decay model that starts with a distribution in strength, one might want to know given an initial strength, when a given specimen will fail. This is particularly important in Monte Carlo simulations where samples can be randomly selected from the distribution in strengths to determine the resulting distribution in failure times. A proposed stress history might become complex, as shown in figure 3.

Equation 12 predicts the time to failure for a constant stress period. The equation was derived in reference 7 by assuming that failure will occur when the strength equals the current stress level. Therefore, eq. 12 results from setting $s[t]$ equal to σ in eq. 4.

$$t_f = c\left(\left(\frac{s_o}{\sigma}\right)^b - 1\right) \tag{12}$$

For a constant ramp from zero stress, $\sigma[t] = R\ t$. Equation 13 is derived by setting the applied load equal to the instantaneous strength but cannot be solved as a simple closed form expression for t_f.

$$R\ t_f = \left(s_0^b - \frac{t_f(R\ t_f)^b}{c(1+b)}\right)^{1/b} \tag{13}$$

Similarly, eq. 14 is the expression for failure after a ramp from an arbitrary load. The equation is only slightly more complicated than eq. 13, but it too cannot not be easily expressed as a closed form expression for t_f.

$$\sigma_1 + R(t_\mathrm{f} - t_1) = \left(s_1^b - \frac{(R(t_\mathrm{f}-t_1)+\sigma_1)^{1+b} - (R\ t_1+\sigma_1)^{1+b}}{c(1+b)R}\right)^{1/b} \tag{14}$$

Two methods for solving the problem are suggested: the "forward" solution, and the "backward" solution.

FORWARD SOLUTION

The forward solution solves eq. 14 iteratively. First, check to see if a failure occurred in the ramp period by using eq. 15.

$$\sigma_1 < s_1\ and\ \ \sigma_2 > s_2 \tag{15}$$

If eq. 15 is satisfied, then sometime during the ramp from t_1 to t_2, the stress exceeded the strength, and a failure occurred, resulting in the need to determine the precise time to failure. If eq. 15 is not satisfied, then no failure occurred, and a failure in a subsequent loading period can be explored.

To solve for a failure in the ramp from t_1 to t_2, one should solve for the root of eq. 16, which is just a reformatted version of eq. 14.

$$F[\mathrm{t}] = \sigma_1 + R(\mathrm{t} - t_1) - \left(s_1^b - \frac{(R(\mathrm{t}-t_1)+\sigma_1)^{1+b} - (R\ t_1+\sigma_1)^{1+b}}{c(1+b)R}\right)^{\frac{1}{b}} = 0 \tag{16}$$

A solution for the root of $F[t]$ can be found using the following iteration (Newton's Method),

$$t_{i+1} = t_i - \frac{F[t_i]}{F'[t_i]} \tag{17}$$

Because b can be large (i.e., 100 to 150), eq. 17 can be slow to converge. To speed convergence, a change of variables is suggested. Let $x = \left(\frac{\sigma_1 + R(t - t_1)}{s_1}\right)^b$ and $A = c(1+b)R$ which leads to

$$x_{i+1} = x_i - \frac{\frac{x_i}{A}\left(A + s_1 x_i^{1/b}\right) - 1 - \frac{\sigma_1}{A}\left(\frac{\sigma_1}{s_1}\right)^b}{1 + \left(1 + {}^1/_b\right)\frac{s_1}{A} x_i^{1/b}} \tag{18}$$

Starting with $x_o = (s_2/s_1)^b$, t_f and s_f can be calculated from the converged solution using

$$s_f = s_1(x)^{1/b} \quad \text{and} \quad t_f = t_1 + \frac{s_1(x)^{1/b} - \sigma_1}{R} \tag{19}$$

Note that if R is positive, slightly faster convergence can be attained by letting x_o=1.

BACKWARD SOLUTION

The forward solution solved for t_f given an initial strength, but an iterative solution was required. If one starts with a specified value of t_f , the equations can be rewritten to work backwards to the required initial strength and then to the reliability prediction using eq. 5. This method may also allow one to concentrate on predictions where the chances of failure are small without a large number of Monte Carlo simulations.

Equations 4 and 10 can be reformulated as eq. 20 and 21 to calculate s_1, given s_2. One can work backwards from a failure point where $t_f = t_2$ and $\sigma = s_2$, through a complex load history, to the initial strength in the first loading period, where $s_o = s_1$.

Constant stress: $$s_1 = \sigma\left(\left(\frac{s_2}{\sigma}\right)^b + \frac{(t_2 - t_1)}{c}\right)^{1/b} \tag{20}$$

Ramp: $$s_1 = \left(s_2^b + \frac{(t_2 - t_1)\left(R(t_2 - t_1)\right)^b}{c(1+b)}\right)^{1/b} \tag{21}$$

One additional check however must be made. Although eq. 20 and 21 will calculate the initial strength required for failure at the proposed time, they cannot determine whether a failure could have occurred earlier in the load history. Figure 4 shows strength degradation predictions for a proof loading case assuming two different initial strengths. Using eq. 20 and 21, a normal failure at t =0.019 hr. would require an initial strength, s_o=0.987. However, using the same equations, failures at 0.0025, 0.003 and 0.01 hr. would all require an initial strength of s_o=0.982. Since a test specimen can only fail once, it would have already failed by the time it reached 0.01 hr. To protect against identifying a fictitious failure, one should check the end of each previous load step to insure that $\sigma_2 < s_2$. If a previous failure occurred, there will not be a future failure, and the originally proposed failure time is part of a safe period. In Figure 4, again the T1000/epoxy material parameters were used as presented earlier, but the stress levels shown are highly elevated above what would normally be used to better illustrate the nature of the strength decay.

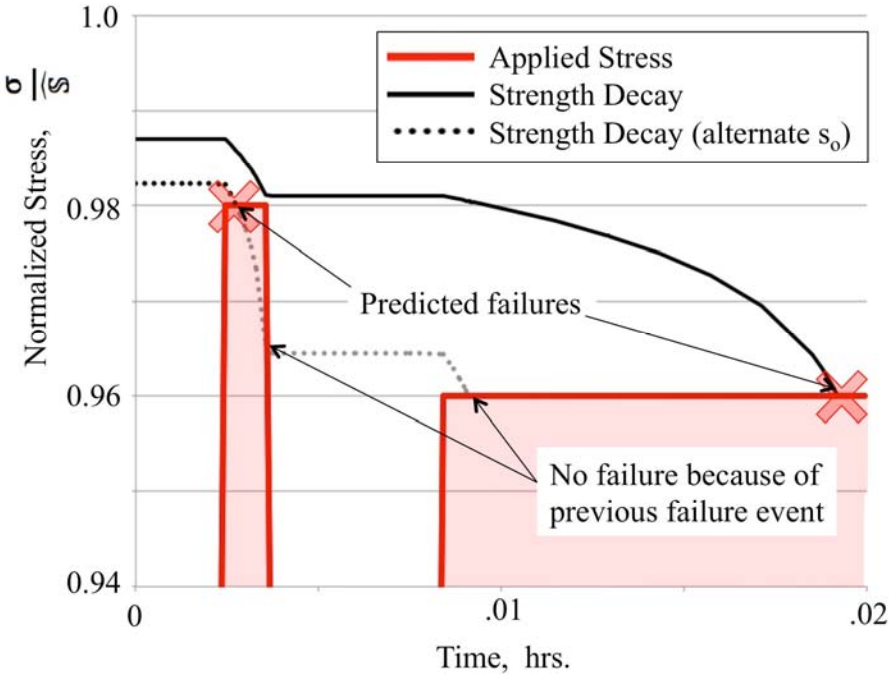

Figure 4. Strength decay with proof loading

IMPLICATIONS OF RAMPS ON RELIABILITY PREDICTIONS

Implications for Initial Strength

The extension of the strength decay model to include ramps may seem like a small adjustment to the model, but it has a few important consequences. One implication involves the interpretation of initial strength. In the original formulation without ramps, the initial strength was assumed to be the measured nominal strength from tests. But strength tests are not instantaneous jumps to failure, they are normally constant ramp tests as shown in Figure 5. The time scale of the ramp is normally small compared to the time scale at which stress rupture tests are conducted. With the strength decay model, the strength of the material is dropping very quickly as the stress approaches the strength value. The ramp rate may not be fast in comparison to this drop in strength. Therefore, the difference in initial strength to the strength that can be measured in a test may be significant, especially since the time-to-failure can be quite sensitive to the initial strength. When the time-to-failure in strength testing is known, eq. 22 can be used to correct the measured strength to more accurately predict the initial strength of the material. Measured strength is characterized by the nominal value and the spread. Since a Weibull distribution in initial strength is assumed, the nominal strength is the Weibull scale parameter, and the spread is characterized by the shape parameter. Figure 5 shows that the drop in strength during a constant ramp test is similar for a range of initial strength values. Because the drop in strengths is similar, the spread of the distribution may not be significantly affected.

$$\widehat{\mathbb{S}}_{true} = \widehat{\mathbb{S}}_{measured}\left(1 + \frac{t_f}{c(1+b)}\right)^{1/b} \tag{22}$$

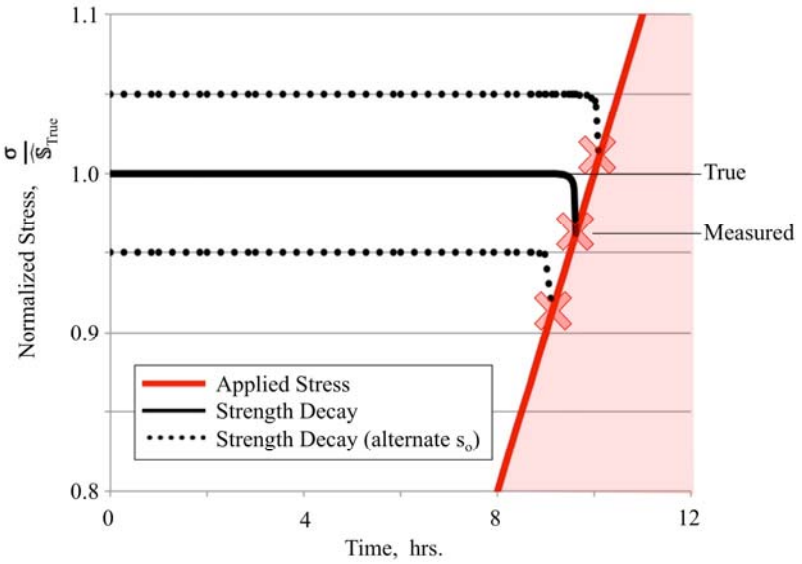

Figure 5. Strength decay while testing for strength

When comparing the classic model to the decay model, one additional correction should be made. If the classic model uses $\widehat{\mathbb{S}}_{measured}$ and the decay model uses $\widehat{\mathbb{S}}_{true}$, the models will give different results for large values of *t*, unless *c* is also corrected as given by

$$c = t_{ref}\left(\frac{\widehat{\mathbb{S}}_{true}}{\widehat{\mathbb{S}}_{measured}}\right)^{b} \tag{23}$$

This correction is only needed when trying to make direct comparisons between the classic and decay models. Otherwise, *c* is determined by fitting to experimental results from stress rupture tests. For the T1000 parameters being used in this paper, the two corrections are $\widehat{\mathbb{S}}_{true} = 1.0022\ \widehat{\mathbb{S}}_{measured}$ and b =0.78 t_{ref} for a 2 minute strength test.

Implications for decreasing load periods

A second consequence for the inclusion of ramps in the model occurs when unloading. If loading and unloading occur instantaneously, then no change in strength is predicted due to the unloading and reloading. A change in strength caused by the loading and unloading might seem like a small effect because the time spent loading and unloading is normally small. However, by neglecting it, a safe period is always predicted when going from a higher load level to a lower load level. The safe period is predicted because of the modeling assumption that it takes time for a strength value that did not fail at the higher level to drop to the lower stress level. Figure 6 shows a proof loading case with a slow ramp rate. With the ramp included in the model, it is clear that, depending on the ramp rate and the material parameters, a failure may occur during the unloading or reloading periods. Notice that the failures on unloading and reloading require almost identical initial strengths. The probability, therefore, of having precisely the correct initial strength to cause one of these failures would be low but finite. When failures during unloading are possible, no safe period would be predicted during the subsequent constant load period. These failures are only possible when the strength falls faster than the unloading rate. This implies that, to preserve the

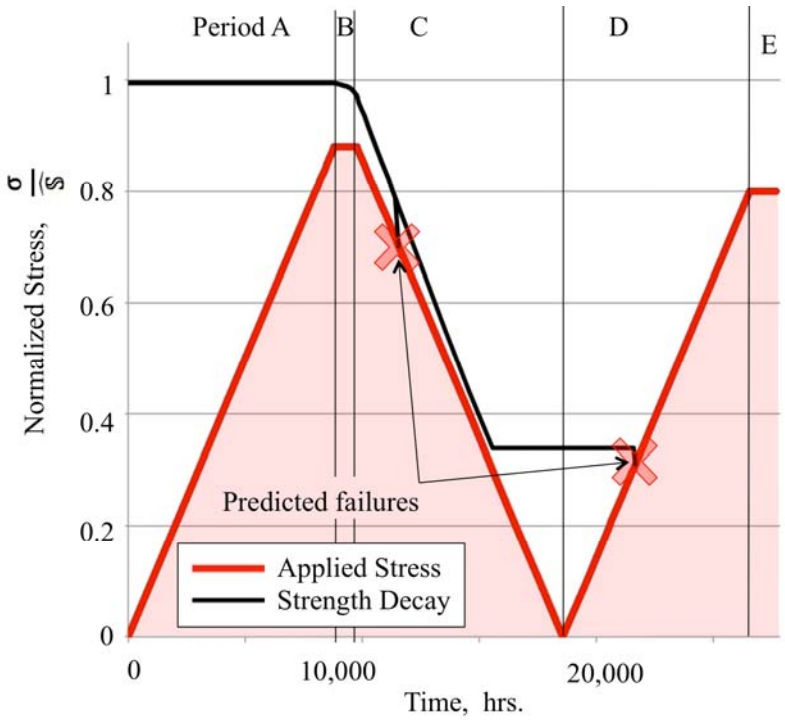

Figure 6. Modeling showing failures on unloading or reloading are possible

safe period, unloading more quickly is desirable. To preserve the possibility of a safe period, one would want to assure that the unloading rate is faster than

$$|R| > \frac{\sigma}{bc} \tag{24}$$

This equation was derived from eq. 7 by assuming the stress level and strength were the same at the end of the hold period and calculating the rate of change in strength. If the unloading rate is faster, then the strength and the load level will move apart as the ramp occurs, and the rate of strength change will decrease. If the ramp rate is slower, it is possible for the strength to decrease faster than the decreasing stress level, making a failure on unloading possible and negating a safe period on reloading.

Implications for failures on loading

When testing for stress rupture, the stress level must be elevated to obtain a reasonable number of failures in a reasonable amount of time. Because of the elevated loading levels, some specimens can be expected to fail on loading. With instantaneous loading assumed in the original formulation, predictions of reliability had to somehow account for these early failures. This complicated the modeling because the initial loading was not actually modeled. By including the loading ramps, failures on loading can be treated just as failures predicted in any other part of the load history making the model more consistent.

EXAMPLE RELIABILITY PREDICTIONS

The strength decay model was introduced to help understand the effects of proof loading. The inclusion of ramps provides a realistic model with which to predict the reliability following proof loads. Tests can be planned to distinguish between the decay model and the classic model when predicting the effect of proof loading on the continued reliability of composite materials. Testing for the effect of proof is difficult for several reasons. Reliability testing, even without proof, is conducted at highly elevated loads. With proof, there is little room to elevate the nominal test level before strength failures would be predicted. Even if one can apply a proof load without breaking the specimen, there is concern about whether this load, which would need to be very close to the strength level, could create damage that is not characteristic of a normal proof loading. A normal proof load would be at a level that is significantly less than the strength. Second, proof loading is generally effective at significantly reducing the failure rate; therefore it can be difficult to plan an experiment where enough failures are obtained to see a significant difference between models. Although models may predict fairly close reliabilities under conditions that can be tested, the model predictions can still be quite different when the models are used to extrapolate to lower stress levels where real structures are used.

The strength decay model is appealing because it can predict a safe period where failures are not possible and a means to extrapolate higher stress level testing to lower level stress testing. In the following three test cases, reliability predictions of the classic model will be compared to the expanded strength decay model.

Case 1. Ramp to Constant Load

Figure 7 compares predictions of reliability from the classic model to the predictions from the expanded decay model for a simple ramp and hold load case.

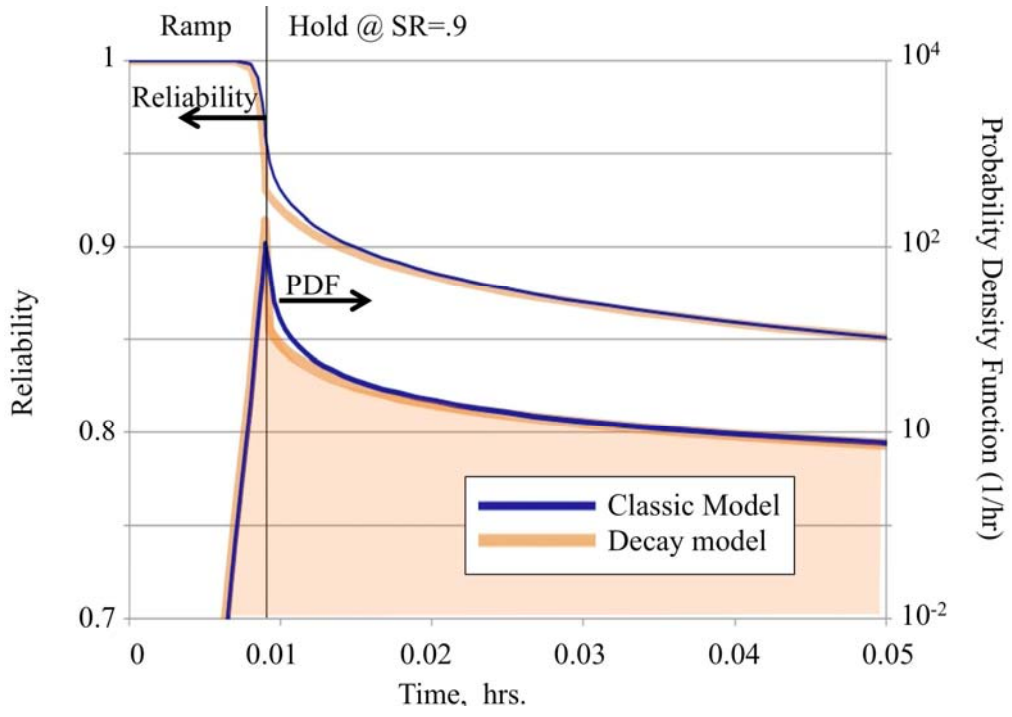

Figure 7. Comparison of model reliability predictions

The parameters used in the model are for the T1000/epoxy as discussed earlier, but the decay model parameters were corrected to account for the difference between measured and true initial strength as discussed earlier in the paper. The *c* value is therefore equal to 0.00078 hr. Although the true nominal strength is used in the decay reliability calculations, the figure presents the stress level as a stress ratio, SR, which is the stress level normalized by the measured nominal strength. This normalization allows a direct comparison of the two models for a consistent stress level.

The reliability prediction for the classic model was calculated from eq. 2, and the reliability prediction from the strength decay model is from eq. 5 once the initial strength has been determined, given a failure at some point in time. The reliability predictions are the fraction of tests that are expected to survive to a given time and are always constant or decreasing since the number of failures cannot decrease with time. In test planning, it can also be helpful to consider the probability density function (*PDF*), which is the likelihood of failures occurring at a specific point in time. A simple finite difference method is used here to estimate the *PDF* as given in eq. 25 for both the classic and decay predictions.

$$PDF = \frac{\mathbb{R}[t] - \mathbb{R}[t+\Delta t]}{\Delta t} \tag{25}$$

Note that because the *PDF* can vary widely in magnitude, it is plotted on a log scale as shown on the right hand axis of Figure 7. From the figure, it is clear that the two models are very close for the simple ramp and hold case and that the *PDFs* for both models drop very quickly from the point where the sample first reaches the maximum load. There are subtle differences between the models in the region where the hold begins. The decay model predicts slightly more failures at the end of the ramp and fewer failures at the very beginning of the hold region. Very quickly, both the *PDF* and the reliability predictions become indistinguishable. This trend continued for a very long time beyond the plotted time period.

Case 2. Proof loading

The second example case presents a proof load as shown in Figure 8, where a short elevated stress level is followed by a longer hold at a lower stress level. In this example the elevated *SR* is 0.9 followed by a *SR* of 0.88. The reliability plots for the two models appear identical. However, the *PDF* plot is more sensitive to small changes in reliability. By looking at the *PDF* plot, subtle differences between the models can be detected at the very end of the ramp to proof load, and a significant difference can be seen in the hold following proof. Notice that for this case the decay model predicts a safe period. In the safe period, the *PDF* for the decay model is zero because no failures occur, which means that the reliability prediction is constant during this period. In the ramp down after proof and back up, the classic model predicts a very low probability of failure that is too low to be plotted on the graph. The only significant difference between the two models is in the safe period, which only lasts for a short period of time (about 0.1 hr. after reaching 0.88 *SR*). The classic model predicts a *PDF* in the same time period of around 0.008 1/hr. Because the time is short and the *PDF* is low, the classic model predicts a low probability of failures occurring in the safe period. A test program to detect a difference between a low probability of failure and no probability of failure would require a large number of test specimens. A better way of testing is needed.

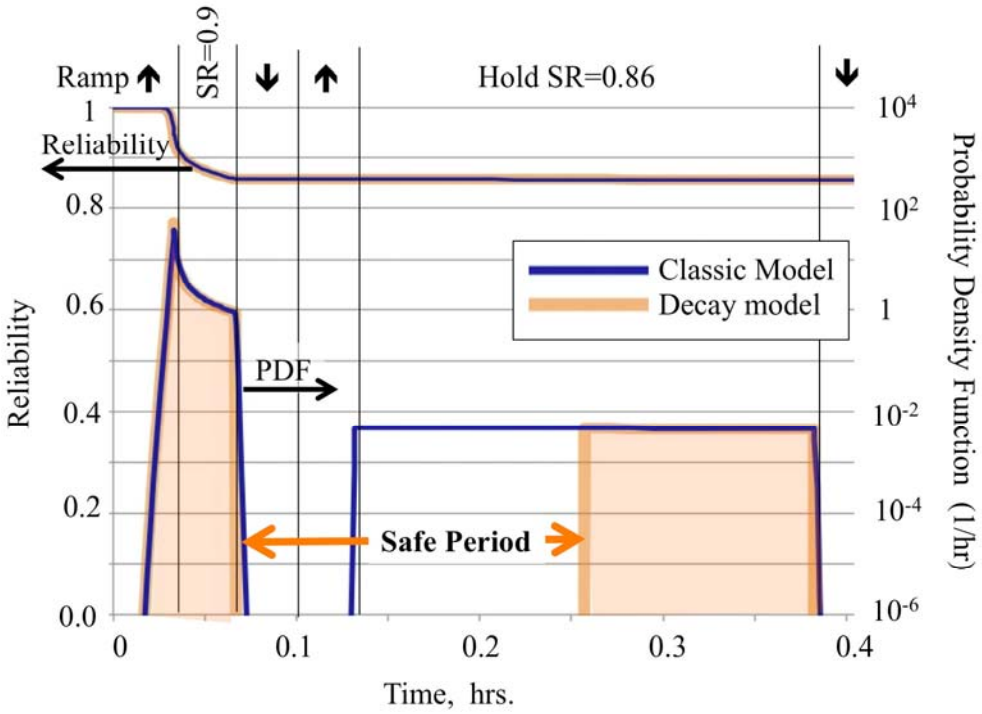

Figure 8. Proof loading reliability predictions

It is important to realize that although in this example the safe period is short, with actual proof loads in current use, the safe periods could be quite long. The predicted safe period using the same material parameters but with a proof level of *SR*=0.75 followed by loading at a *SR* =0.5 would be 10^{13} years. If this safe period could be trusted, then COPVs could be designed to be more efficient and still have plenty of safe life.

Case 3. Multistep testing

Given the results of the example case 2, it is clear that testing in the safe period is critical to differentiate the two models. However, under elevated stress conditions, the safe period can be quite short, and the expected failures from the classic model is also quite small. To accentuate the differences in the models and to maximize the use of a limited number of test specimens, a series of increasing proof loads followed by holds at a reduced load level is suggested, as shown in Figure 9. The figure shows significant drops in reliability during the proof periods indicating that most failures occur during these load excursions. By choosing a hold time at the reduced stress level longer than the safe period, each safe period is followed by a time where the two models are in close agreement. In this example, the first proof is at *SR*=0.9 which results in about 10% of the specimens failing. The hold period is 3% below the proof load and results in a safe period that is only a few minutes long. With each succeeding load series, both the proof level and the following holds are raised by 2%. By summing the expected number of failures in all the safe periods and comparing them to the expected failures in the later portion of the holds, a clear difference in the models can be detected with a reasonable number of test specimens. With the proposed testing, the classic model would predict that a total of 2.5% of the specimens

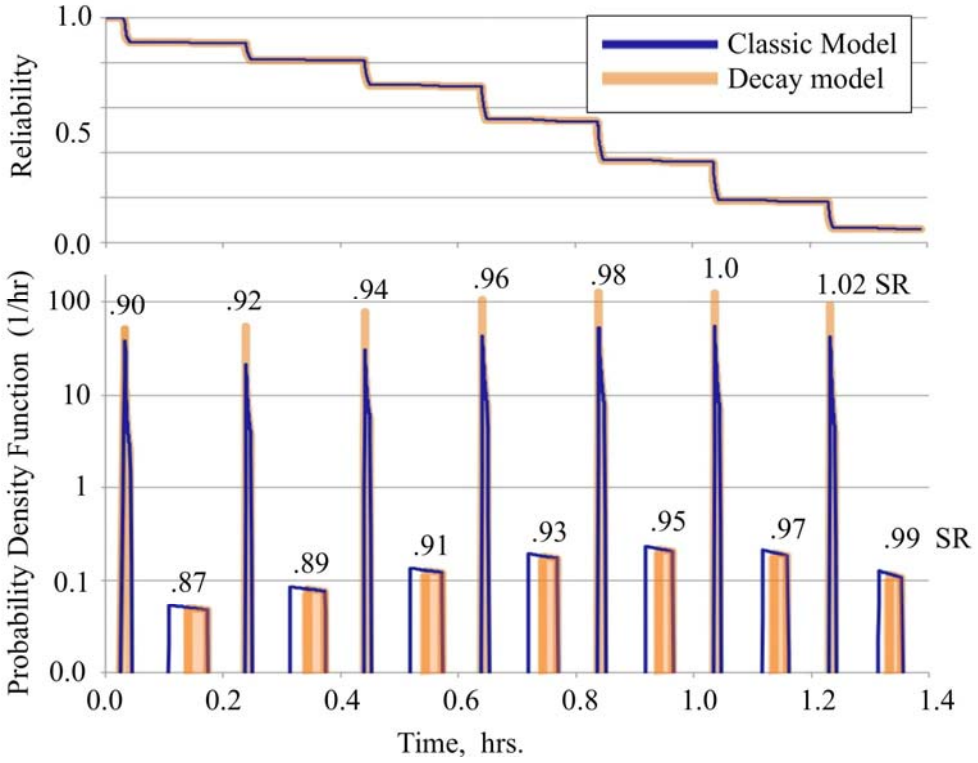

Figure 9. Reliability predictions for proposed multistep proof test

would fail during the seven safe periods and an additional 2.5% would fail during the second half of the holds. The decay model would predict no failures during the safe period and 2.5% during the second half of the hold. This multistep loading procedure provides a reasonable test that could be conducted with one or two hundred test specimens. Failures during the safe periods provide a clear distinction between the models, and the failures during the second half provide a control to ensure that the material properties used in the models are providing appropriate predictions. This example shows how complicated it can be to plan a test series that adequately measures the effect of proof loading. If the proof load is elevated too far above the subsequent holds, too few failures would be predicted following the proof. If the loading ramps are too long, then failures could occur during the ramps and no safe period would exist. Models such as this expanded decay model are critical to planning successful tests to characterize and capitalize on the true nature of the material.

Conclusion

Stress rupture is a critical failure mode for certain composite structures such as composite overwrap pressure vessels, and concerns about stress rupture significantly limit the structural efficiency of these structures. A previously proposed reliability model for stress rupture is based on strength decay in the material over time and assumes that failure occurs when the reduced strength equals the loading level. The previously proposed model was limited to constant stress level loading periods but was expanded here to include arbitrary load histories. The inclusions of linear ramps, in combination with constant load periods, allows much more realistic load histories to

be modeled than was previously possible. The time-to-failure during a ramp period could not be solved in closed form so two solution techniques were suggested: (i) choose a proposed initial strength and solve for the time to failure using an iterative solution; (ii) choose a time-to-failure and work backwards to the required initial strength. The second solution can be solved in closed form but must be checked to insure that the specimen did not fail at some previous point in time. If failure at a given time requires a certain initial strength, but a specimen with that strength would have previously failed, then no failures can occur at the originally proposed time, indicating a safe period. These safe periods are a feature of this decay model and, if validated, could lead to more efficient structures while still maintaining the required level of safety. Testing for safe periods to validate this type of model, however, is quite difficult because alternate models predict low, but finite, probabilities of failure following proof loads. To validate the model, a series of increasing proof loads, followed by lower stressed holds, is suggested. This provides an efficient use of the test specimens even though most of the test specimens will still fail during the proof loads. The inclusion of ramps in the model also highlighted that there may be a difference between the initial strength assumed in the model and the strength that can be measured during testing. A correction can be made for this difference. Yet another issue associated with the inclusion of the ramps in the model is that if the loading ramps (particularly the unloading ramp) are too slow, then the safe period may be significantly reduced or eliminated. The strength decay model ties the distribution in initial strengths to stress rupture failures and provides a consistent model for the two types of tests. By including ramps in the decay model, failures that occur during the initial loading ramp can be modeled as any other failure.

References

1. Shaffer, J.T. 1986. "Stress Rupture of Carbon Fiber Composite Materials," in 18th International SAMPE Conference, Seattle WA.
2. Cameron, K.D. et al. 2006. "Shelf Life Phenomenon and Stress Rupture Life of Carbon/Epoxy Composite Overwrapped Pressure Vessels," NASA Engineering and Safety Center, RP-06-83.
3. Grimes-Ledesma, L., et al. 2012. "Composite Pressure Vessel Working Group (CPVWG) Task 3: Stress Rupture Test Approach," NASA Engineering and Safety Center, RP-09-00537.
4. Phoenix, S.L. and L.N.P. Murthy. 2007. "Pros and Cons of Proof Testing Carbon Composite Overwrapped Pressure Vessels: A Comparison of Two Mathematical Models," in 48th AIAA/ASME/ASCE/AHS/ASC Structures, Structural Dynamics, and Materials Conference, Long Beach, CA.
5. Outwater, J. O. and W. J. Seibert. 1963. “On The Strength Degradation of Filament Wound Pressure Vessels Subjected to a History of Loading,” University of Vermont, Technical Memorandum No. 196.
6. Reeder, J.R., 2010. "A Critique of a Phenomenological Fiber Breakage Model for Stress Rupture of Composites Materials," NASA Langley Research Center, NASA TM-2010-216721.
7. Reeder, J.R. 2012. "Composite Stress Rupture: A New Reliability Model Based on Strength Decay," NASA Langley Research Center, NASA TM-2010-217566.